Dalton Transactions

RSC Publishing

COMMUNICATION

View Article Online
View Journal | View Issue

Reactivity comparison of high-valent iron(IV)-oxo complexes bearing *N*-tetramethylated cyclam ligands with different ring size†

Cite this: *Dalton Trans.*, 2013, **42**, 7842

Received 20th March 2013,
Accepted 28th March 2013

DOI: 10.1039/c3dt50750e

www.rsc.org/dalton

Seungwoo Hong,‡[a] Hee So,‡[a] Heejung Yoon,[a,b] Kyung-Bin Cho,[a] Yong-Min Lee,[a] Shunichi Fukuzumi*[a,b] and Wonwoo Nam*[a]

The ring size effect of macrocyclic TMC ligands in nonheme iron(IV)-oxo complexes has been examined in hydrogen atom transfer (HAT) and oxygen atom transfer (OAT) reactions; an iron(IV)-oxo complex bearing a smaller TMC ligand is more reactive in both HAT and OAT reactions, resulting from its high $Fe^{IV/III}$ redox potential.

High-valent iron(IV)-oxo intermediates have been identified as reactive species in the catalytic cycles of dioxygen activation by mononuclear nonheme iron enzymes.[1] In biomimetic studies, a crystal structure of a mononuclear nonheme iron(IV)-oxo complex bearing an *N*-tetramethylated cyclam (TMC) ligand, $[Fe^{IV}(O)(14\text{-TMC})(CH_3CN)]^{2+}$ (**1**, 14-TMC = 1,4,8,11-tetramethyl-1,4,8,11-tetraazacyclotetradecane; see Chart 1 for the structure of **1**) was reported for the first time in 2003.[2] Since then, a number of iron(IV)-oxo complexes have been synthesized using various supporting ligands, characterized by various spectroscopic techniques and X-ray crystallography, and investigated in the oxidation of organic substrates and electron transfer reactions.[3–5] It has also been shown that reactivities of the nonheme iron(IV)-oxo complexes in oxygen atom transfer (OAT), hydrogen atom transfer (HAT), and electron transfer (ET) reactions are markedly affected by the supporting ligands (*e.g.*, TMC derivatives and tripodal tetradentate N4 and pentadentate N5 ligands),[6] the identity of the axial ligand coordinated to the iron(IV) center in the *trans*-position to the oxo ligand,[7] the structure and spin state of iron(IV)-oxo complexes,[8] and the binding of redox-inactive metal ions by the iron-oxo moiety.[9]

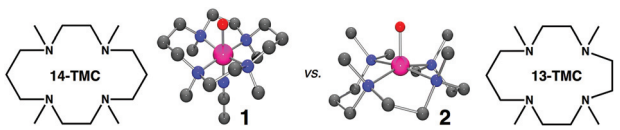

Chart 1

Recently, we reported the synthesis of metal–dioxygen complexes ($M–O_2$) bearing TMC ligands and demonstrated that the ring size of the TMC ligands is an important factor in regulating the geometric and electronic structures of the $M–O_2$ complexes (*e.g.*, side-on $M^{(n+1)+}$-peroxo *vs.* end-on M^{n+}-superoxo).[10] For example, a side-on Ni(III)-peroxo complex is formed with a 12-TMC ligand (12-TMC = 1,4,7,10-tetramethyl-1,4,7,10-tetraazacyclododecane), whereas a 14-TMC ligand affords an end-on Ni(II)-superoxo complex.[11] More recently, we have shown the formation of Ni(II)-superoxo and Ni(III)-peroxo complexes bearing a common macrocyclic 13-TMC ligand (13-TMC = 1,4,7,10-tetramethyl-1,4,7,10-tetraazacyclotridecane).[12] In addition, the nucleophilic reactivity of the $M–O_2$ complexes in aldehyde oxidation and O_2-transfer reactions was markedly dependent on the ring size of the TMC ligands in metal-peroxo complexes.[11,13]

Despite the aforementioned significant ring size effects on $M–O_2$ complexes bearing TMC ligands, the oxidizing reactivity of iron(IV)-oxo complexes bearing TMC ligands with different ring size, $[Fe^{IV}(O)(n\text{-TMC})]^{2+}$, has yet to be examined to clarify the origin of the difference in the reactivity.[14] We report herein synthesis of an iron(IV)-oxo complex bearing a 13-TMC ligand, $[Fe^{IV}(O)(13\text{-TMC})]^{2+}$ (**2**, see Chart 1 for the DFT-optimized structure of **2** and ESI,† DFT Calculation section), which was well characterized by various spectroscopic methods. The successful synthesis and characterization of **2** has led us to compare the reactivity of **1** and **2** in HAT and OAT reactions; **2** is a much stronger oxidant than **1** in those reactions. The reactivity difference between **1** and **2** is rationalized with their $Fe^{IV/III}$ redox potentials; the redox potential of **2** is 0.22 V higher than that of **1**.

The starting $Fe^{II}(13\text{-TMC})(CF_3SO_3)_2$ complex was prepared by reacting $Fe^{II}(CF_3SO_3)_2$ and 13-TMC in CH_3CN (see ESI, Experimental section and Fig. S1†). Addition of 1.5 equiv. of

[a]*Department of Bioinspired Science, Department of Chemistry and Nano Science, Ewha Womans University, Seoul 120-750, Korea. E-mail: wwnam@ewha.ac.kr*
[b]*Department of Material and Life Science, Osaka University and ALCA (JST), 2-1 Yamada-oka, Suita, Osaka 565-0871, Japan. E-mail: fukuzumi@chem.eng.osaka-u.ac.jp*

†Electronic supplementary information (ESI) available: Experimental and kinetic details. See DOI: 10.1039/c3dt50750e

‡These authors contributed equally to this work.

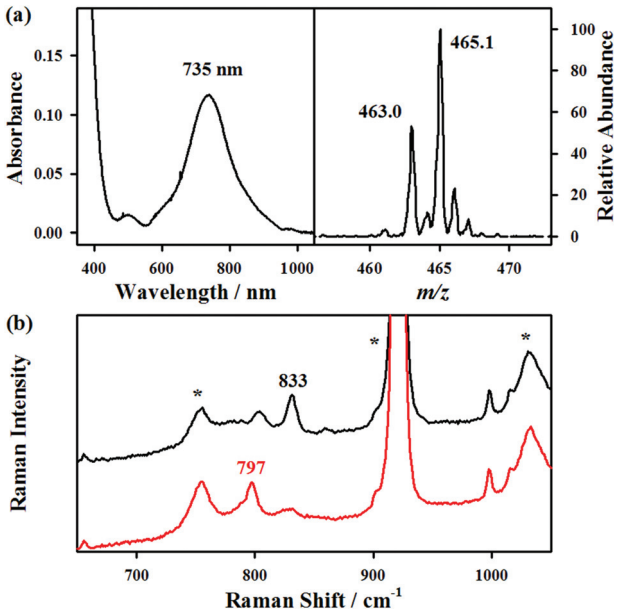

Fig. 1 (a) UV-vis spectrum of **2** (0.5 mM) in CH_3CN at −40 °C (left panel) and ESI-MS of **2**-^{16}O (m/z = 463.0) and **2**-^{18}O (m/z = 465.1) (right panel). (b) rRaman spectra of **2**-^{16}O (black) and **2**-^{18}O (red) upon 407 nm excitation in CH_3CN at −40 °C.

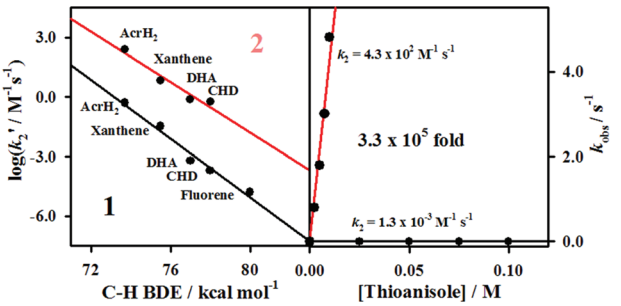

Fig. 2 Plots of log k'_2 against the substrates C–H BDE for **1** (black line) and **2** (red line) in CH_3CN at −40 °C (left panel). All k_2 values were then adjusted for the reaction stoichiometry to yield k'_2 values based on the number of equivalent target C–H bonds in the substrate (also see ESI, Table S1†). Right panel shows plots of k_{obs} against thioanisole concentrations for **1** (black line) and **2** (red line) in CH_3CN at −40 °C. Temperature-dependent kinetics were examined for **1** in order to estimate k_2 values at −40 °C (also see ESI, Fig. S5 and Table S1†).

iodosylbenzene (PhIO) to a solution containing $[Fe^{II}(13\text{-TMC})]^{2+}$ afforded a green intermediate **2**, which was metastable in CH_3CN at −40 °C ($t_{1/2} \approx 30$ min). The UV-vis spectrum of **2** exhibits an absorption band at 735 nm with a low extinction coefficient (ε = 240 M^{-1} cm^{-1}), characteristic of mononuclear nonheme iron(IV)-oxo complexes (Fig. 1a, left panel).[2–4] The electrospray ionization mass spectrum (ESI-MS) of **2** exhibits a prominent isotope sensitive ion peak centered at m/z 463.0 (ESI, Fig. S2†), whose mass and distribution patterns correspond to $[Fe^{IV}(O)(13\text{-TMC})(CF_3SO_3)]^+$ (*calcd* m/z 463.1). Upon addition of PhI^{16}O to a solution containing $[Fe^{II}(13\text{-TMC})]^{2+}$ and a small amount of $H_2{}^{18}O$, ESI-MS of **2** exhibits two ion peaks at m/z 463.0 and 465.1 (Fig. 1a, right panel), which are assigned to $[Fe^{IV}(^{16}O)(13\text{-TMC})(CF_3SO_3)]^+$ (**2**-^{16}O; *calcd* m/z 463.1) and $[Fe^{IV}(^{18}O)(13\text{-TMC})(CF_3SO_3)]^+$ (**2**-^{18}O; *calcd* m/z 465.1). Upon 407 nm excitation in CH_3CN at −40 °C, the resonance Raman (rRaman) spectrum of **2**-^{16}O shows one isotopically sensitive band at 833 cm^{-1}, which shifts to 797 cm^{-1} upon ^{18}O-substitution (Fig. 1b). The observed isotopic shift of −36 cm^{-1} with ^{18}O-substitution is in good agreement with the calculated value ($\Delta\nu_{calcd}$ = −37 cm^{-1}) for the Fe–O diatomic harmonic oscillator.[14,15] The X-band EPR spectrum of **2** is silent, as observed in other nonheme iron(IV)-oxo complexes.[2–4] Based on the spectroscopic characterization presented above, **2** is assigned unambiguously as an iron(IV)-oxo complex bearing a 13-TMC ligand, $[Fe^{IV}(O)(13\text{-TMC})]^{2+}$ (**2**).

The reactivity of **2** was investigated in HAT reactions with a series of substrates having a weak C–H bond dissociation energy (BDE), such as 10-methyl-9,10-dihydroacridine ($AcrH_2$; 73.7 kcal mol^{-1}), xanthene (75.5 kcal mol^{-1}), 9,10-dihydroanthracene (DHA; 77 kcal mol^{-1}), and 1,4-cyclohexadiene (CHD; 78 kcal mol^{-1}) in CH_3CN at −40 °C (ESI, Table S1†). The reaction rates monitored by the disappearance of the absorption band at 735 nm obeyed pseudo-first-order kinetics (ESI, Fig. S3†). The second-order rate constants, determined from the slope of the first-order rate constants (k_{obs}) against substrate concentrations (ESI, Fig. S4†), decreased with an increase of C–H BDE of substrates (Fig. 2, left panel). A significant kinetic isotope effect (KIE) of 36 was obtained in the oxidation of xanthene and xanthene-d_2 (ESI, Fig. S5†); such large KIE values were usually observed in the C–H bond activation of alkanes by nonheme iron(IV)-oxo complexes.[6a,7,8a] In the oxidation of DHA and CHD by **2**, anthracene (45%) and benzene (47%) were obtained as sole products under an Ar atmosphere, respectively. The iron product in the final reaction solutions was also analysed with EPR and ESI-MS. An X-band EPR spectrum of the reaction solution of **2** and CHD exhibited signals at g = 7.6, 6.9, 5.7, 5.3 and 4.3 (ESI, Fig. S6†), characteristic of high-spin Fe^{III} species (S = 5/2). Upon addition of 1,1,-dimethylferrocene (Me_2Fc) to the resulting solution, the EPR spectrum became silent (ESI, Fig. S6†), indicating that the Fe^{III} species was reduced by Me_2Fc to give an Fe^{II} species. In ESI-MS experiments, we observed ion peaks at m/z of 157.5 and 464.0 in the reaction solution of **2** and CHD (ESI, Fig. S7a†); the peaks correspond to $[Fe^{III}(OH)(13\text{-TMC})]^{2+}$ (*calcd* m/z 157.6) and $[Fe^{III}(OH)(13\text{-TMC})(CF_3SO_3)]^+$ (*calcd* m/z 464.1). Reduction of the Fe^{III} species by Me_2Fc afforded ESI-MS showing two prominent ion peaks at m/z of 169.5 and 447.2 corresponding to $[Fe^{II}(13\text{-TMC})(CH_3CN)]^{2+}$ (*calcd* m/z 169.6) and $[Fe^{II}(13\text{-TMC})(CF_3SO_3)]^+$ (*calcd* m/z 447.1), respectively (ESI, Fig. S7b†). Based on the spectroscopic analysis of the iron product formed in the oxidation of CHD by **2**, we conclude that an Fe^{III} species, not an Fe^{II} species, is formed as the major product and that the C–H bond activation does not occur *via* an oxygen-rebound mechanism as we reported recently.[16]

The reactivity of **1** in HAT reaction was also investigated to compare with that of **2**. Due to the low reactivity of **1**,

temperature-dependent kinetic studies for **1** were performed to estimate its reactivity at −40 °C (ESI, Table S1 and Fig. S8†). The results indicate that **2** is ~3.0×10^3 times more reactive than **1** at −40 °C, confirming that **2** is more reactive than $[Fe^{IV}(O)(N4Py)]^{2+}$ (N4Py = *N*,*N*-bis(2-pyridylmethyl)-*N*-bis(2-pyridyl)methylamine) and $[Fe^{IV}(O)(TBC)]^{2+}$ (TBC = 1,4,8,11-tetrabenzyl-1,4,8,11-tetraazacyclotetradecane).[17]

The reactivities of **1** and **2** were also compared in OAT reactions, using thioanisole as a substrate in CH_3CN at −40 °C. Upon addition of thioanisole to the solutions of **1** and **2**, the $Fe^{IV}(O)$ intermediates reverted back to the starting Fe^{II} complexes, yielding methyl phenyl sulfoxide quantitatively (ESI, Table S1 and Fig. S9†).[16b] Second order rate constants of 1.3×10^{-3} for **1** and 4.3×10^2 for **2** were obtained from the plots of pseudo-first-order rate constants against thioanisole concentrations (Fig. 2, right panel; ESI, Fig. S8d and S10†), indicating that the reactivity of **2** is $>10^5$ fold greater than that of **1** in the oxidation of thioanisole. Again, **2** is more reactive than $[Fe^{IV}(O)(N4Py)]^{2+}$ and $[Fe^{IV}(O)(TBC)]^{2+}$ in OAT reactions.[17]

We then carried out ET reactions between **2** and Fc derivatives to determine the $Fe^{IV/III}$ redox potential of **2**.[6b] Upon addition of bromoferrocene (BrFc, E_{ox} value of 0.54 V *vs.* SCE) to the solution of **2** in CH_3CN at −40 °C, the absorption band at 735 nm decreased with the concurrent appearance of an absorption band at 675 nm due to the bromoferrocenium ion ($BrFc^+$; λ_{max} = 675 nm and ε = 320 M^{-1} cm^{-1}) (ESI, Fig. S11†). The amount of $BrFc^+$ formed implies that a one-electron transfer reaction occurs between **2** and BrFc. We also found that the ET between **2** and BrFc is in equilibrium [eqn (1)], where the final concentration of $BrFc^+$ produced in the ET reduction of **2** increased with an increase in the initial concentration of BrFc (ESI, Fig. S12†). The equilibrium constant (K_{et}) was determined to be 28 at −40 °C by fitting the plot (see ESI,† Experimental section for spectral redox titration). The apparent one-electron reduction potential of **2** was then determined to be E_{red} = 0.61 V *vs.* SCE, with the K_{et} value of 28 and the E_{ox} value of BrFc (0.54 V *vs.* SCE) using the Nernst equation [eqn (2)].

$$BrFc + [Fe^{IV}(O)(13\text{-TMC})]^{2+} \overset{K_{et}}{\rightleftharpoons} BrFc^+ + [Fe^{III}(O)(13\text{-TMC})]^+ \quad (1)$$

$$E_{red} = E_{ox} + (RT/F)\ln K_{et} \quad (2)$$

Since the E_{red} value of **1** reported previously was determined at 25 °C (E_{red} = 0.39 V *vs.* SCE),[6b] we carried out the redox titration of **1** with Fc at −40 °C. We found that the ET between **1** and Fc was in equilibrium,[6b] and the equilibrium constant (K_{et}) was determined to be 2.5 (ESI, Fig. S13†). The E_{red} of 0.39 V *vs.* SCE at −40 °C for **1** was then obtained using the Nernst equation [eqn (2)] with the K_{et} value of 2.5 and the E_{ox} value of Fc (0.37 V *vs.* SCE). These results indicate that the E_{red} of **2** is 0.22 V more positive than that of **1** and even higher than those of other $Fe^{IV}(O)$ complexes such as $[Fe^{IV}(O)(N4Py)]^{2+}$ (0.51 V *vs.* SCE at 25 °C) and $[Fe^{IV}(O)(Bn\text{-}TPEN)]^{2+}$ (0.49 V *vs.* SCE at 25 °C; Bn-TPEN = *N*-benzyl-*N*,*N*′,*N*′-tris(2-pyridylmethyl)ethane-1,2-diamine).[6b]

In summary, we have synthesized a nonheme iron(IV)-oxo complex bearing a 13-membered TMC ligand. By comparing reactivities of iron(IV)-oxo complexes bearing different TMC ligands, we found that $[Fe^{IV}(O)(13\text{-TMC})]^{2+}$ is much more reactive than $[Fe^{IV}(O)(14\text{-TMC})]^{2+}$ in both HAT and OAT reactions, demonstrating that the ring size of the TMC ligands is an important factor that determines the oxidizing power of nonheme iron(IV)-oxo complexes. The reactivity difference of the iron(IV)-oxo complexes is rationalized with their $Fe^{IV/III}$ redox potentials; the reduction potential of $[Fe^{IV}(O)(13\text{-TMC})]^{2+}$ is 0.22 V greater than that of $[Fe^{IV}(O)(14\text{-TMC})]^{2+}$.

This work was supported by NRF/MEST of Korea through CRI, GRL (2010-00353), and WCU (R31-2008-000-10010-0) and a Grant-in-Aid (no 20108010) from MEXT, Japan (to S.F.).

Notes and references

1 (*a*) E. I. Solomon, T. C. Brunold, M. I. Davis, J. N. Kemsley, S.-K. Lee, N. Lehnert, F. Neese, A. J. Skulan, Y.-S. Yang and J. Zhou, *Chem. Rev.*, 2000, **100**, 235; (*b*) D. P. Galonić, E. W. Barr, C. T. Walsh, J. M. Bollinger Jr. and C. Krebs, *Nat. Chem. Biol.*, 2007, **3**, 113; (*c*) C. Krebs, D. G. Fujimori, C. T. Walsh and J. M. Bollinger Jr., *Acc. Chem. Res.*, 2007, **40**, 484; (*d*) P. C. A. Bruijnincx, G. van Koten and R. J. M. K. Gebbink, *Chem. Soc. Rev.*, 2008, **37**, 2716.

2 J.-U. Rohde, J. In, M. H. Lim, W. W. Brennessel, M. R. Bukowski, A. Stubna, E. Münck, W. Nam and L. Que Jr., *Science*, 2003, **299**, 1037.

3 (*a*) W. Nam, *Acc. Chem. Res.*, 2007, **40**, 522; (*b*) S. P. de Visser, J.-U. Rohde, Y.-M. Lee, J. Cho and W. Nam, *Coord. Chem. Rev.*, 2013, **257**, 381.

4 (*a*) J. Hohenberger, K. Ray and K. Meyer, *Nat. Commun.*, 2012, **3**, 720; (*b*) A. R. McDonald and L. Que Jr., *Coord. Chem. Rev.*, 2013, **257**, 414.

5 S. Fukuzumi, *Coord. Chem. Rev.*, 2013, **257**, 1564.

6 (*a*) J. Kaizer, E. J. Klinker, N. Y. Oh, J.-U. Rohde, W. J. Song, A. Stubna, J. Kim, E. Münck, W. Nam and L. Que Jr., *J. Am. Chem. Soc.*, 2004, **126**, 472; (*b*) Y.-M. Lee, H. Kotani, T. Suenobu, W. Nam and S. Fukuzumi, *J. Am. Chem. Soc.*, 2008, **130**, 434; (*c*) P. Comba, S. Fukuzumi, H. Kotani and S. Wunderlich, *Angew. Chem., Int. Ed.*, 2010, **49**, 2622; (*d*) M. S. Seo, N. M. Kim, K.-B. Cho, J. E. So, S. K. Park, M. Clémancey, R. Garcia-Serres, J.-M. Latour, S. Shaik and W. Nam, *Chem. Sci.*, 2011, **2**, 1039; (*e*) S. Hong, Y.-M. Lee, K.-B. Cho, K. Sundaravel, J. Cho, M. J. Kim, W. Shin and W. Nam, *J. Am. Chem. Soc.*, 2011, **133**, 11876; (*f*) W. Ye, D. M. Ho, S. Friedle, T. D. Palluccio and E. V. Rybak-Akimova, *Inorg. Chem.*, 2012, **51**, 5006; (*g*) D. Wang, K. Ray, M. J. Collins, E. R. Farquhar, J. R. Frisch, L. Gómez, T. A. Jackson, M. Kerscher, A. Waleska, P. Comba, M. Costas and L. Que Jr., *Chem. Sci.*, 2013, **4**, 282; (*h*) N. Ségaud, J.-N. Rebilly, K. Sénéchal-David, R. Guillot, L. Billon, J.-P. Baltaze, J. Farjon, O. Reinaud and F. Banse, *Inorg. Chem.*, 2013, **52**, 691.

7 C. V. Sastri, J. Lee, K. Oh, Y. J. Lee, J. Lee, T. A. Jackson, K. Ray, H. Hirao, W. Shin, J. A. Halfen, J. Kim, L. Que Jr., S. Shaik and W. Nam, *Proc. Natl. Acad. Sci. U. S. A.*, 2007, **104**, 19181.

8 (*a*) J. England, M. Martinho, E. R. Farquhar, J. R. Frisch, E. L. Bominaar, E. Münck and L. Que Jr., *Angew. Chem., Int. Ed.*, 2009, **48**, 3622; (*b*) D. C. Lacy, R. Gupta, K. L. Stone, J. Greaves, J. W. Ziller, M. P. Hendrich and A. S. Borovik, *J. Am. Chem. Soc.*, 2010, **132**, 12188; (*c*) J. P. Bigi, W. H. Harman, B. Lassalle-Kaiser, D. M. Robles, T. A. Stich, J. Yano, R. D. Britt and C. J. Chang, *J. Am. Chem. Soc.*, 2012, **134**, 1536.

9 (*a*) S. Fukuzumi, Y. Morimoto, H. Kotani, P. Naumov, Y.-M. Lee and W. Nam, *Nat. Chem.*, 2010, **2**, 756; (*b*) J. Park, Y. Morimoto, Y.-M. Lee, W. Nam and S. Fukuzumi, *J. Am. Chem. Soc.*, 2011, **133**, 5236.

10 (*a*) J. Cho, R. Sarangi and W. Nam, *Acc. Chem. Res.*, 2012, **45**, 1321; (*b*) J. Cho, S. Jeon, S. A. Wilson, L. V. Liu, E. A. Kang, J. J. Braymer, M. H. Lim, B. Hedman, K. O. Hodgson, J. S. Valentine, E. I. Solomon and W. Nam, *Nature*, 2011, **478**, 502.

11 (*a*) J. Cho, R. Sarangi, J. Annaraj, S. Y. Kim, M. Kubo, T. Ogura, E. I. Solomon and W. Nam, *Nat. Chem.*, 2009, **1**, 568; (*b*) M. T. Kieber-Emmons, J. Annaraj, M. S. Seo, K. M. Van Heuvelen, T. Tosha, T. Kitagawa, T. C. Brunold, W. Nam and C. G. Riordan, *J. Am. Chem. Soc.*, 2006, **128**, 14230.

12 J. Cho, H. Y. Kang, L. V. Liu, R. Sarangi, E. I. Solomon and W. Nam, *Chem. Sci.*, 2013, **4**, 1502.

13 J. Cho, R. Sarangi, H. Y. Kang, J. Y. Lee, M. Kubo, T. Ogura, E. I. Solomon and W. Nam, *J. Am. Chem. Soc.*, 2010, **132**, 16977.

14 Y. Suh, M. S. Seo, K. M. Kim, Y. S. Kim, H. G. Jang, T. Tosha, T. Kitagawa, J. Kim and W. Nam, *J. Inorg. Biochem.*, 2006, **100**, 627.

15 (*a*) C. V. Sastri, M. J. Park, T. Ohta, T. A. Jackson, A. Stubna, M. S. Seo, J. Lee, J. Kim, T. Kitagawa, E. Münck, L. Que Jr. and W. Nam, *J. Am. Chem. Soc.*, 2005, **127**, 12494; (*b*) Y.-M. Lee, S. N. Dhuri, S. C. Sawant, J. Cho, M. Kubo, T. Ogura, S. Fukuzumi and W. Nam, *Angew. Chem., Int. Ed.*, 2009, **48**, 1803.

16 (*a*) K.-B. Cho, X. Wu, Y.-M. Lee, Y. H. Kwon, S. Shaik and W. Nam, *J. Am. Chem. Soc.*, 2012, **134**, 20222; (*b*) X. Wu, M. S. Seo, K. M. Davis, Y.-M. Lee, J. Chen, K.-B. Cho, Y. N. Pushkar and W. Nam, *J. Am. Chem. Soc.*, 2011, **133**, 20088.

17 S. A. Wilson, J. Chen, S. Hong, Y.-M. Lee, M. Clémancey, R. Garcia-Serres, T. Nomura, T. Ogura, J.-M. Latour, B. Hedman, K. O. Hodgson, W. Nam and E. I. Solomon, *J. Am. Chem. Soc.*, 2012, **134**, 11791.